

Gas-Phase Photoemission Investigation of Diethynylthiophene: Experiment and Theory

Giovanni Polzonetti,^{*,†} Giorgio Contini,[‡] Vincenzo Carravetta,[§] Claudio Lo Sterzo,^{||}
Antonella Ricci,^{||} Angelica Ferri,[⊥] Stefano Stranges,[⊥] and Monica de Simone[†]

Department of Physics and Unità INFM and INSTM, University "Roma Tre", Via della Vasca Navale 84, I-00146 Rome, Italy, CNR-ISM, Via Fosso del Cavaliere, 100-00133 Rome, Italy, CNR-IPCF, Via Moruzzi 1, 56124 Pisa, Italy, CNR-Institute of Chemistry of Organometallic Compounds (ICCOM-CNR), Department of Chemistry, University "La Sapienza" P. le A. Moro, 5-00185 Rome, Italy, and Department of Chemistry, University "La Sapienza" P. le A. Moro, 5-00185 Rome, Italy

Received: August 1, 2002; In Final Form: March 3, 2003

The photoelectron (PE) and X-ray absorption (NEXAFS) spectra of gaseous diethynylthiophene (DET) at the C 1s and S 2p core levels are presented and discussed. The NEXAFS spectra have been obtained in the total-ion-yield mode. The ionization energies have been determined for C 1s and S 2p spectra by Δ SCF calculations, while the NEXAFS spectra, at both the C K-edge and S L-edge, have been simulated by STEX calculations. Good agreement between experiment and theory is generally observed. A strong perturbation of the electronic structure of thiophene at the α - and β -carbon atoms, induced by the two ethynyl substituents, is inferred by the analysis of the spectra.

Introduction

The electronic structure of five-membered aromatic heterocyclic compounds is of great interest since these species form the basis for a series of organic conducting polymers.¹ These materials, possessing the peculiarity of a long chain conjugation backbone, are attracting considerable attention from several scientific communities, because of their application as components of electronic devices. At present, one branch of these activities seems to outgrow basic research, as the first technological applications are becoming real. Traditionally used semiconducting materials are currently being replaced with organic compounds in some specific applications, for instance, FET (field emission transistor) and LED (light-emitting devices). The low cost, processability, and versatility are, among the others, the parameters that make these materials convenient and advantageous for replacing the traditional ones.

Electrochemically synthesized polymers such as polythiophene,² polypyrrole,^{3,4} and polyaniline⁴ have been investigated as they become semiconductors upon doping and show a relatively high degree of stability in air, ultrahigh vacuum, and organic solvents. In the recent past, the addition of 3-alkyl side chains was introduced in an effort to improve the processability of the polymer, allowing production of workable conducting polymers.⁵

In this framework, several oligomers and polymers of thiophene, a five-membered aromatic heterocyclic hydrocarbon containing sulfur, have been synthesized and investigated. The obtained materials have been extensively studied and conveniently used for FET^{6,7} and LED^{8–10} realization; however, the basic understanding of many of the chemical and physical

aspects still must be investigated. To expand opportunities offered by thiophene-containing conjugated polymers, new synthetic routes leading to structures bearing ethyne groups and metal centers inserted between thiophene rings have been developed¹¹ as shown hereafter. The spacing of the thiophene rings with the electron-rich acetylide and metal center moieties should result in the enhancement of both electron density and conjugation, and thus delocalization, throughout the polymer chain and, consequently, their related properties.

Several investigations on thiophene, model systems, and polymers based on thiophene have been performed.^{12–18} More recently, we investigated by photoelectron spectroscopy¹⁹ some of the synthesized materials in an effort to obtain a better definition of both the chemical and electronic structure of diethynylthiophene and Pt- and Pd-containing oligomers.

In this paper, we report additional information from this research program, which leads to elucidation of the electronic structure of the basic, thiophene-containing organic spacer diethynylthiophene (DET) (see Figure 1 for the molecular structure), synthesized and used in our laboratory. Synchrotron radiation-induced photoelectron (PE) and near-edge X-ray absorption fine structure (NEXAFS) spectroscopies, carried out under gas-phase conditions, have been used in this study to probe the electronic structure of both occupied and unoccupied orbitals. Δ SCF (self-consistent field) calculations have been employed to estimate the core ionization energy for each chemically different carbon atom and for the sulfur atom of DET. The *ab initio* STEX method²⁰ has been used for the calculation of the NEXAFS spectra at either the C K- or S L-edge.

Experimental Section

The experiments have been performed at the gas-phase photoemission beamline of the third-generation storage ring ELETTRA (Trieste, Italy). PES spectra have been recorded with a 50 mm mean radius VSW hemispherical electron analyzer, with a four-element lens system with one single channeltron

* To whom correspondence should be addressed. E-mail: polzonet@uniroma3.it.

[†] University "Roma Tre".

[‡] CNR-ISM.

[§] CNR-IPCF.

^{||} CNR-Institute of Chemistry of Organometallic Compounds (ICCOM-CNR), Department of Chemistry, University "La Sapienza" P. le A. Moro.

[⊥] Department of Chemistry, University "La Sapienza" P. le A. Moro.

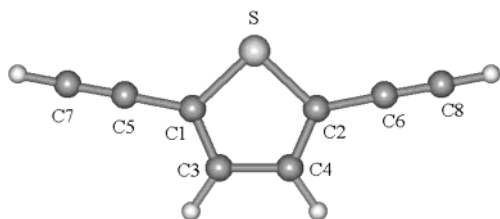


Figure 1. Diethynylthiophene (DET) molecular structure. The labeling of the carbon atoms is used in the text.

electron multiplier, giving a total instrumental (monochromator and analyzer) resolution of 0.4 eV. The analyzer has been used in the constant pass energy mode, with the pass energy set to 25 eV. For the C 1s and S 2p core level PE spectra, photon energies of 337.0 and 190.0 eV, respectively, have been used, with monochromator entrance and exit slits of 30 and 120 μm , respectively. Calibration of the energy scale has been carried out by introducing suitable gases (Ar and SF₆) into the ionization region together with the sample and recording a photoelectron spectrum at the same photon energy.

NEXAFS measurements have been taken in the total-ion-yield mode, by using a time-of-flight mass spectrometer. Calibration of the photon energy scale has been achieved with the Ar 2p_{3/2} \rightarrow 4s absorption line at 244.3 eV,²¹ for the carbon core edge, and the S 2p absorption peak of SF₆ at 178.63 eV²² for the S L-edges. All NEXAFS spectra are normalized to the incident photon flux as measured just after the ionization chamber.

The position of the electron spectrometer for the PE experiments was kept at the “magic angle” (54.7°) with respect to the polarization vector of the synchrotron radiation. The total-ion-yield (NEXAFS) spectra were collected in the direction of the light polarization vector. The base pressure in the vacuum chamber was in the low 10⁻⁵ Pa range.

The synthesis of 2,5-diethynylthiophene (H-C \equiv C-Ar-C \equiv C-H, Ar being thiophene) (see Figure 1) has been performed by modification of the reported reaction procedure.^{11a,23} The DET, after syntheses, was stored in a series of sealed vials under an argon atmosphere, and constantly kept at -60 °C (dry ice). Vials were opened immediately prior to use and introduced into a CF16-flanged glass vessel connected to the gas line by a leak valve. The DET sample which is solid at low temperatures (<0 °C), albeit with a high vapor pressure, was constantly kept in a thermostatic bath at -16 °C for all the measurements. Before the measurements were taken, the glass vessel was pumped down; successively, the sample was transferred into the vessel under an argon atmosphere and isolated by a valve. Removal of contaminants was achieved by several cycles of pumping and cooling of the glass vessel, verifying the DET purity by a mass spectrum and valence PE band using 25 eV of photon energy (*hν*). Curve fitting analysis of the C 1s PE spectrum core level was carried out using the Levenburg–Marquardt nonlinear minimization algorithm with nonapproximated Voigt functions.

Computational Details

The geometry of DET has been computed by ground state SCF optimization with a basis set of triple- ζ quality. The calculations of the ionization energies for all the chemically inequivalent carbon atoms and sulfur were performed in the Δ SCF approximation by using the DALTON code.²⁴ The set of excitation energies and corresponding oscillator strengths, obtained by STEX²⁰ calculations for each C site, were instead used to obtain the absorption cross section.

Calculations of the reference ground and core-ionized states were carried out employing triple- ζ plus polarizing and diffuse function basis sets on C and S atoms and double- ζ basis sets on H atoms. After the double-basis set algorithm had been adopted, the STEX Hamiltonian was then calculated, adding to this basis set a large number of diffuse functions to give an augmented basis set. The Stieltjes imaging technique²⁵ was applied to the discretized STEX spectrum in the continuum, and the resulting spectrum was then convoluted with a Gaussian function with a full width at half-maximum (fwhm) of 0.4 eV to simulate the effect of both the limited experimental resolution and the vibrational broadening of the bands in the discrete energy region with the purpose of making the comparison with the experimental data easier. The use of a Gaussian function here is, evidently, an approximation. The effective vibrational line shape of a NEXAFS peak can be, in principle, more complex and asymmetric, thus producing a different distribution of intensity. A careful investigation, adopting a basis set with increasing size and improving quality, has been performed to verify that both the computed PE spectrum and the computed NEXAFS spectra that are presented do not show any basis set dependence. When electron correlation effects and the effect of screening of the excited electron are neglected, STEX is evidently more suitable for those excited states that can be reasonably described by “single excitations”, and, among those, for high-energy excited states of Rydberg or continuum character. For the lowest-valence character of the core excited states, the missing screening may result in energy errors of \sim 1–2 eV; this error can be generally assumed to be similar for the different excitation channels, leading to a common compression of the “discrete” core excitations toward the ionization threshold. In the case of the S L-edge, the spin-orbit coupling leading to a splitting of the excitations complicates the theoretical analysis. This has been empirically simulated by the duplication of the STEX spectrum computed without taking into account explicitly the effect of the spin-orbit coupling. More precisely, we obtained the full spectrum as the superposition of two spectra shifted by 1.20 eV (PE experimental spin-orbit splitting), assuming a statistical value of 2–1 for the relative intensities of the L_{3/2} and L_{1/2} channels. It should be added that the S 2p level is molecular field split into quasi-degenerate sublevels that are accessible by the Δ SCF approximation. The interaction between the corresponding excitation subchannels is, however, neglected in the STEX-independent channel approximation adopted here.

Results and Discussion

Photoelectron (PE) Spectra. C 1s PE Spectra. The C 1s experimental photoelectron spectrum of gaseous DET and the best fit, obtained using four Voigt peaks and the linear background, are presented in Figure 2. The ionization energy, amplitude, and widths of the four Voigt functions in the fit were treated as free parameters (Voigt widths and amplitude were shared between the four components). The residual between the experimental data and the fit is also reported. To allow an easier comparison between experiment and theory, Figure 2 also reports the calculated bar diagram for the four (see Figure 1 for numbering) chemically inequivalent carbon atoms.

The experimental spectrum appears as a broad band; however, the four components could be resolved using a fit procedure. The ionization energy (IE) values determined by the fitting analysis for the four C 1s components are 290.48, 290.86, 291.27, and 291.72 eV as reported in Table 1, with a slight increase in energy spacing (0.38, 0.41, and 0.45 eV, respectively)

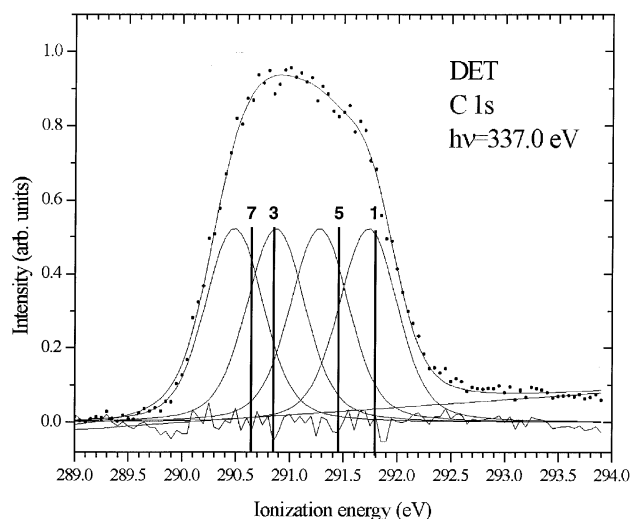


Figure 2. Carbon 1s PE experimental spectrum of DET vapor obtained using a photon energy of 337.0 eV. The experimental spectrum (dots) is shown together with the best fit obtained using four Voigt functions and a linear background (see the text for details); the residual between the experimental data and the fit is also reported. The bars correspond to the results of computations for the four (see Figure 1 for numbering) chemically inequivalent carbon atoms.

TABLE 1: Experimental Ionization Energies (IEs), for Gas-Phase DET, from PE Spectra for the C 1s (as obtained by the best fit) and S 2p Core Levels and Energy Position of the Transitions as Detected in the Total-Ion-Yield (NEXAFS) C K-Edge and S L-Edge Spectra^a

C atom	S atom
C 1s PE	S 2p PE
290.48 (0)	169.95 2p _{3/2}
290.86 (0.38)	171.15 2p _{1/2}
291.27 (0.79)	
291.72 (1.24)	
C K-edge	S L-edge
284.76	165.48
285.45	166.64
285.73	167.43
286.41	168.17
287.43	168.53
289.2	169.56
293.4	171.0
296.1	173.9
302.0	
309	

^a For C 1s PE data, the energy shift relative to the lowest ionization energy value is shown in parentheses.

and a total energy separation between the first and the last peak of 1.24 eV. From simple chemical and physical considerations, we expect that the carbon atoms bonded either to the sulfur or to the acetylene group will experience the strongest charge withdrawal by their neighbors, with the result being that they have the highest IE values.

To obtain more accurate hints about the C 1s PE spectral contributions, Δ SCF calculations of the ionization energies (IEs) for the optimized molecular structure of DET have been performed, and the resulting IEs, for the four chemically inequivalent carbon atoms, C₁, C₃, C₅, and C₇ (see Figure 1), are presented as a bar diagram in Figure 2 (see also Table 2). By comparison with the IE values obtained by the fit of the C 1s PE experimental spectrum (see Figure 2 and Table 1), we observe a good overall agreement between experiment and theory that allows the correct assignment of the four different C 1s contributions to the spectrum. The low-energy spectral

TABLE 2: Theoretical Results^a

C K-edge	S L-edge
C ₁	lower series (2p _{3/2})
287.59 (0.0307) (a'')	166.48 (0.00310) (a'')
289.80 (0.0085) (a')	166.50 (0.00090) (a'')
290.18 (0.0017) (a')	167.49 (0.00758) (a')
290.61 (0.0010) (a')	167.77 (0.01204) (a')
290.96 (0.0013) (a'')	167.91 (0.00053) (a')
291.80 IE	168.61 (0.00051) (a')
C ₃	168.63 (0.00744) (a')
287.04 (0.0272) (a'')	169.03 (0.00053) (a')
288.56 (0.0018) (a')	169.09 (0.00051) (a')
289.13 (0.0061) (a'')	169.40 (0.00139) (a'')
289.39 (0.0058) (a'')	169.50 (0.00075) (a'')
289.76 (0.0030) (a'')	169.57 (0.00150) (a'')
290.87 IE	169.66 (0.00084) (a'')
C ₅	170.03 (0.00050) (a')
287.74 (0.0202) (a'')	170.25 IE
288.44 (0.0344) (a')	upper series (2p _{1/2})
290.08 (0.0037) (a'')	167.68 (0.00155) (a'')
290.50 (0.0019) (a'')	168.69 (0.00379) (a')
290.61 (0.0034) (a'')	168.97 (0.00602) (a')
290.94 (0.0037) (a'')	169.83 (0.00372) (a')
291.46 IE	170.14 (0.00067) (a')
C ₇	170.60 (0.00070) (a'')
286.86 (0.0215) (a'')	170.77 (0.00075) (a'')
288.23 (0.0244) (a')	171.45 IE
288.29 (0.0040) (a')	
288.79 (0.0018) (a')	
288.92 (0.0013) (a')	
288.92 (0.0016) (a'')	
289.39 (0.0011) (a')	
289.86 (0.0017) (a'')	
290.28 (0.0011) (a')	
290.31 (0.0013) (a'')	
290.62 IE	

^a Main STEX excitation energies (below the ionization thresholds) and oscillator strengths (in parentheses) at the C K-edge and S L-edge of DET. For the C K-edge, the four channels (C₁, C₃, C₅, and C₇) due to the four inequivalent carbon atoms are included. For the S L-edge, the two channels, due to the 2p_{3/2} and 2p_{1/2} core levels, are included. Δ SCF ionization thresholds (IEs) and the symmetry of the transitions, in the molecular plane (a') and out of the molecular plane (a''), are also reported.

intensity is due to the ionization of C₇, the carbon atom of the ethynyl groups, as a consequence of the charge transfer from the ring. C₁, on the other hand, experiences a strong charge withdrawal by two of its neighbors, ethyne and sulfur, and therefore is characterized by the lowest charge density and, correspondingly, the highest ionization energy, as expected. C₅ becomes quite positively charged as well, while C₃ exhibits a C 1s ionization energy that is lower and close to that of C₇. Because of the presence of the ethynyl groups in DET, the ionization energies of the carbon atoms of the thiophene ring, bonded (C₁≡C α) and not bonded (C₃≡C β) to sulfur, differ from those of the thiophene molecule. The ionization energy separation between C α and C β for DET is 0.93 and 0.86 eV as derived by calculation and by a fit of the experimental spectrum, respectively.

Thiophene has been investigated in the gas phase by photoelectron spectroscopy by Gelius *et al.*,²⁶ who found ionization energies of 290.5 and 290.2 eV for C α and C β , respectively. The observed energy gap of \sim 0.3 eV between C α and C β was smaller than expected by some *ab initio* calculations,²⁷ but larger relative to calculated and experimental (0.1 eV) values,²⁸ reported by other investigations. Comparing our results for DET with those reported by Gelius *et al.* for thiophene, we observe a shift toward a higher ionization energy for both thiophenic carbons: 1.22 eV for C α and 0.66 eV for

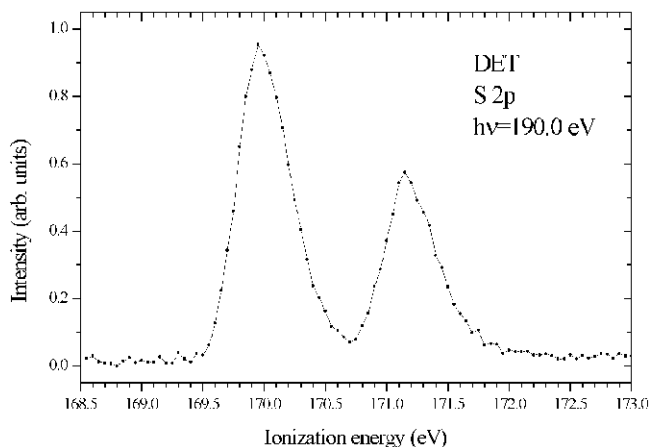


Figure 3. Sulfur 2p PE experimental spectrum of DET vapor obtained with a photon energy of 190.0 eV.

β . A strong perturbation of the electronic structure of the thiophene ring takes place in DET, the α -carbons being more affected, as would be expected on the basis of the chemical structure. By comparing our theoretical values with the C 1s IE value of 291.47 eV calculated for acetylene,²⁹ we observe a negative shift for the IE of C₇ in DET (−0.85 eV) resulting from a more effective electron relaxation around this core hole because of an electron charge withdrawal from the thiophene ring, while for acetylenic C₅ bonded to thiophene, a negligible shift is computed. We have already observed and discussed²⁹ a similar effect in phenylacetylene (PA) in which a negative chemical shift of the binding energies of the alkyne carbons of PA, compared to the acetylene molecule, was found to be as high as −1.35 and −0.68 eV for the ending C1 and for C2 bonded to the benzene ring, respectively. A parallel antiscreening effect was detected for the benzene carbons of PA, mainly for the carbon atom bonded to acetylene, which resulted in a binding energy 0.98 eV higher than that of benzene.

In a previous paper,³⁰ we reported the SR-XPS spectroscopy analysis by experiment and theory of a molecule, diethynylterthiophene (TRIM), made by two ethynyl groups alternating with three thiophene rings, one central and two termini. In the case of TRIM, the C 1s PE spectrum exhibited essentially three peaks at 290.33, 290.59, and 291.43 eV.^{30a}

From the calculated IPs for DET, the energy separation between α - and β -carbons is somehow lower than that for TRIM (0.46 vs 1.1 eV). This can be attributed to the more complex structure in TRIM with a major perturbation of the carbon atoms in the thiophene ring.

More remarkable are the differences relative to the acetylenic carbon atoms when compared to the calculation for acetylene;²⁹ when the acetylenic unit is between two thiophene rings, i.e., TRIM, we compute shifts of −0.51 and −0.44 eV.

S2P PE Spectra. The experimental PE S 2p spectrum showing fully resolved spin–orbit split 3/2 and 1/2 core levels is reported in Figure 3. The peak shape is asymmetric with an fwhm of 0.50 eV for both the S 2p_{3/2} and S 2p_{1/2} components; the energy gap is 1.20 eV. The observed width is larger than the total instrumental broadening (estimated to be less than 240 meV) because of the core-hole lifetime, the vibrational excitations, and the molecular field splitting. Our Δ SCF calculations for DET gave IE values of 170.52 and 170.60 eV for ionization from the perpendicular and in the molecular plane 2p'' orbitals, respectively, corresponding to a molecular field gap of 0.08 eV. The measured S 2p_{3/2,1/2} energy gap is in good agreement with previous reports. For thiophene in the gas phase, Gelius *et al.*²⁶

reported an L_{2,3} line separation of 1.25 eV, and other authors reported a separation of 1.0 eV for solid thiophene.³¹ For polythiophene solid films, a value of 1.2 eV was reported,³² while we found a value of 1.3 eV for organometallic polymers containing thiophene.¹⁹ For the TRIM molecule,³⁰ we measured a value of 1.15 eV, with a broadening of the line width of up to 0.7 eV that was explained by the inequivalency of the sulfur atoms in the molecule.

The S 2p_{3/2} ionization energy value measured for DET is 169.95 eV; Gelius *et al.*²⁶ reported a value of 169.9 eV for thiophene. The difference between the IE of these two molecules is indeed smaller than expected; the charge withdrawal effect of the two ethyne groups is evidently more effective for C₁. For the diethynylterthiophene (TRIM) molecule, we found a value for the S 2p_{3/2} IE of 169.63 eV, the gap being 1.15 eV.³⁰ We might amend the mistake appearing in that paper³⁰ where a value of 169.27 eV has been erroneously published.

Total-Ion-Yield Spectra (NEXAFS). *Carbon K-Edge.* The C K-edge total-ion-yield (NEXAFS) experimental spectrum is displayed in Figure 4. Several structures appear mainly in the lower-photon energy region of the spectrum, as reported in more detail in the top panel of Figure 6. Five main peaks are detected at ~284.8, ~285.4, ~285.7, ~286.4, and 287.4 eV. Additional broad structures at 289, 293, 296, 302, and 309 eV are detected at higher photon energies.

In Figure 5, the C K-edge spectra calculated for DET by the STEX method are displayed. The C K-edge spectrum is reported for each of the four chemically inequivalent carbon atoms of the molecule (C₁, C₃, C₅, and C₇) convoluted in the low-energy region with an fwhm Gaussian function of 0.40 eV, together with the total spectrum (C_{tot}); arrows mark the positions of the core ionization thresholds (IE). Energy transitions and oscillator strengths of the main STEX excitations below the ionization thresholds are also reported in Table 2.

For a better comparison with the experiment, the computed C_{tot} K-edge spectrum is reported with additional information in Figure 6, including details of the low-energy range convoluted profile, and the bar diagram, together with the experimental C K-edge spectrum. This gives both the position in energy and intensity of the main STEX excitations, the labeling giving the relative assignment to the four chemically inequivalent carbon atoms and the symmetry of the transitions, namely, in the molecular plane (*a'*) and out of the molecular plane (*a''*).

The theoretical results reported in Figures 5 and 6 and Table 2 evidence the spectral contributions by each carbon atom and are used for the assignment of the experimental bands. A spectral shape comparison between experiment and theory shows similarities together with some discrepancies in the intensity distribution, particularly in the lower-photon energy region.

In the experimental C K-edge spectrum, the three main low-energy features, labeled in Figure 6 from "a" to "c", appear at 284.8, 285.4, and 285.7 eV with a partial overlap among them. On the basis of calculation, these three resonances are assigned to contributions coming from C₇ and C₃, C₁ and C₅, and C₇ and C₅, respectively. The first two transitions are due to in the molecular plane transitions (*a''*, C 1s → π^*), while the third one is due to out of the molecular plane transitions (*a'*, C 1s → π^*) (see Figure 6 and Table 2).

A careful comparison between the simulated (C_{tot}) and experimental spectra shows that the relative positions of the first three π^* features produce a rather different overall appearance in the C K-edge spectrum, although the relative energy differences are 0.2 eV at maximum. These slight differences in the energy position of the π^* features can be

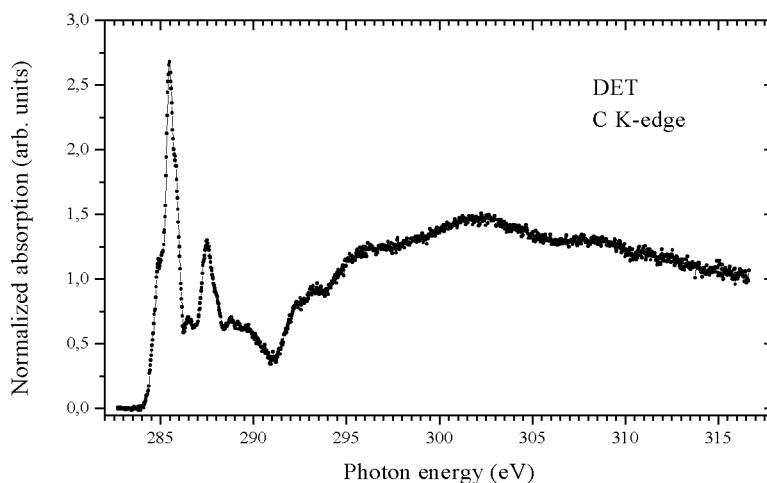


Figure 4. Total-ion-yield (NEXAFS) C K-edge experimental spectrum of DET vapor.

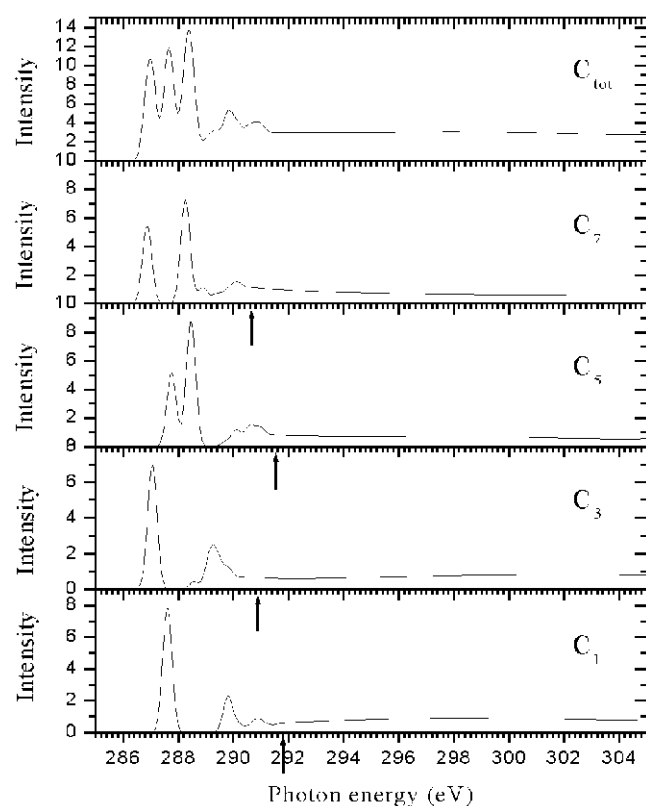


Figure 5. C K-edge spectra calculated by the STEX method for the four inequivalent carbon atoms (C_1 , C_3 , C_5 , and C_7) of DET, convoluted in the low-energy region with 0.40 eV fwhm Gaussian functions. The sum of the four K-edge spectra is denoted C_{tot} . Arrows mark the positions of the core ionization thresholds.

partially due to the approximations in the calculation of the IE values of the C 1s levels, as previously discussed in C 1s PE Spectra. Furthermore, the presence of vibrational progressions in the transition, not taken into account in the calculations presented here, can affect the shape of the total spectrum, as we have already discussed for 2-mercaptobenzoxazole.³³ From this point of view, the convolution with a single Gaussian function of fixed fwhm over the entire energy range, a procedure that we usually adopt for an easier comparison with the experimental data, can also be, on the contrary, misleading. Despite the apparent differences between experiment and theory in the total π^* intensity distribution, transitions “a” and “b” of

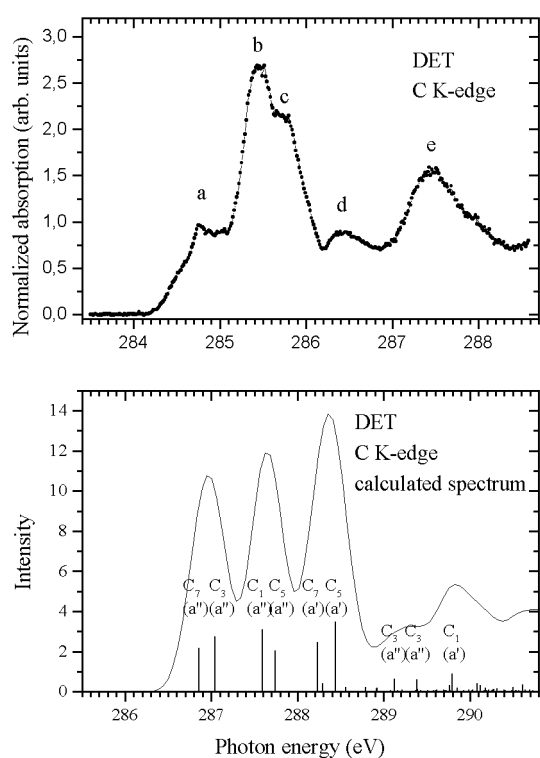


Figure 6. C K-edge spectrum calculated by the STEX method for DET convoluted in the low-energy region with 0.40 eV fwhm Gaussian functions. The figure highlights the low-energy region together with the bar diagram, indicating the energy position and intensity of the main STEX transitions; the assignments of the four carbon atoms and the symmetry of the transitions, namely, in the molecular plane (a') and out of the molecular plane (a''), are also reported. The absolute values of the oscillator strengths (bars) are reported in Table 2. For an easier comparison, the figure also reports the C K-edge experimental spectrum for the low-energy region.

the experimental spectrum are assigned to $1s \rightarrow \pi^*$ core electron transitions by carbon atoms with mostly double bond character and triple-bond plus C–S carbons, respectively, while the “c” feature is assigned to $1s \rightarrow \pi^*$ core electron transitions by carbon atoms with fully triple bond character.

Higher-energy structures found in the theoretical spectrum are caused by an overlapping between transitions derived from different carbon atoms; however, the two features computed at ~ 289.2 and ~ 289.8 eV are mainly due to C_3 (out of the molecular plane symmetry, a'') and C_1 (in the molecular

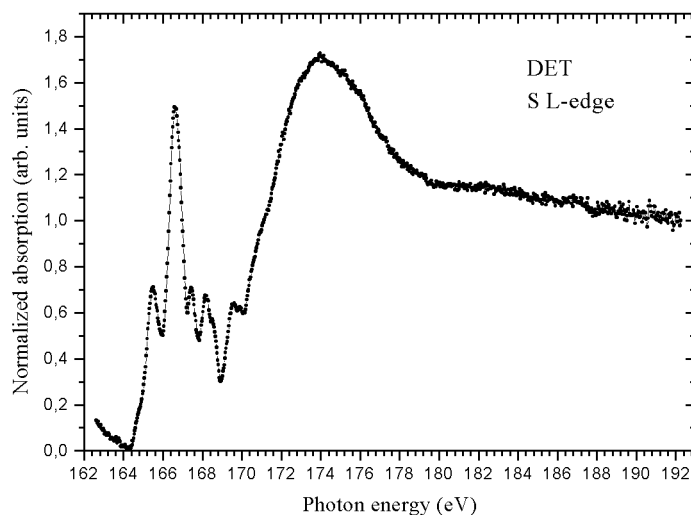


Figure 7. Total-ion-yield S L-edge experimental spectrum of DET vapor.

symmetry, a'), respectively. By experiment, we find a broad envelope that shows the presence of these two structures.

The spectral feature “e” experimentally detected at 287.4 eV is believed to originate from the contribution by the σ^* (C–S bond).

For thiophene in the gas phase, Hitchcock *et al.*¹² have detected only one primary π^* resonance at 285.4 eV derived from both α - and β -carbons (C–S and C–C bonds); one feature at 287.1 eV was assigned to overlapping between σ^* (C–S bond) and π^* (C–C bond), and the shoulder at 288 eV and the feature at 289.3 eV were assigned to the transition to the 3p and 4p levels, respectively. Our experimental (computed) data are generally in agreement with these assignments; however, the differentiation derives from the presence of two ethynyl groups bonded to thiophene, in the present case of DET, which gives rise to several additional contributions, highlighted in the main low-photon energy region with two extra features found at 284.8 (transition “a”) and 285.7 eV (transition “c”).

C₅ and C₇ belonging to the ethyne groups give rise to the π^* level splitting. We have already discussed such an effect^{34,35} as being derived by the reduced symmetry of the acetylene molecule when it is bonded to thiophene. The π^* orbitals, degenerate in the isolated acetylene molecule, will interact differently with the electron distribution of the thiophene ring and can be expected to spawn two energy-separated orbitals. The strong coupling of the π electron systems of the ring and substituent leads to the shift and splitting of the single strong π^* peak observed in spectra of the subunit. This effect is clearly shown in the calculated spectra for these two carbons, where a splitting of approximately 0.6 eV goes together with a significant variation in intensity, which can be rationalized in terms of delocalization of the virtual orbitals.

In the theoretical spectrum, the continuum region does not show any feature above the discussed resonances, although in the C K-edge experimental spectrum, several observable features markedly resemble those of thiophene.¹² Structures are detected at 293, 296, and 302 eV, and a weak structure is detected at 309 eV. According to the molecular structure and literature references, we tentatively assign the features at 293 and 296 eV to the σ^* C–C bond, the broad structure at 302 eV to the σ^* C=C bond, and the weak feature at 309 eV to a σ^* C≡C bond. Vaterlain *et al.*¹³ discussed the C K-edge spectrum for thiophene and also a bithiophene multilayer condensed on Ag-(111) in conjunction with X α -SW calculation data. One main feature was reported at 285.9 eV and assigned to excitation of

the C 1s electrons into the LUMO by both the α - and β -carbons, while the resonance at 287.6 eV was considered to be due to superposition of excitation to the second π^* orbital and the C α –S σ^* orbital; these authors also remark that the feature at 289.5 eV should be considered a mixed valence Rydberg excitation.

Sulfur L-Edge. The S L_{2,3}-edge total-ion-yield (NEXAFS) experimental spectrum is displayed in Figure 7. The lower-photon energy region of the spectrum is reported in more detail in the top panel of Figure 8. The spectrum shows several features at 165.5 eV, very pronounced features at 166.6, 167.4, 168.2, 168.5, and 169.5 eV, a shoulder at \sim 171 eV, and a prominent and broad feature at 173.9 eV. Considering the chemical structure of DET, and taking into account the two contributions at this absorption edge, arising by the two sulfur 2p sublevels 3/2 and 1/2, we can tentatively assign the first spectral feature to an S 2p_{3/2} σ^* resonance, while the second sharp and strong feature should be seen as a superposition of the π^* S2p_{3/2} and σ^* S2p_{1/2} resonances.

The S L-edge-computed spectrum, convoluted with a Gaussian function (fwhm = 0.40 eV), is reported in Figure 8. The full spectrum is shown in the bottom panel, while in the middle panel, the lower-energy region is highlighted together with the bar diagram, describing the energy position and intensity of the main transitions (also reported in Table 2). The arrows mark the position of the core ionization thresholds for the S 2p_{3/2} (bottom) and S 2p_{1/2} (top) channels. For an easier comparison, in the top panel, the S L-edge experimental spectrum is reported for the lower-energy region with labeling of the features from “a” to “g”.

On the theoretical spectrum, obtained as a sum of both S L_{3/2} and L_{1/2} absorption edges, several features appear at 166.5, 167.7, 168.6, and 169.5 eV and a weak feature at 170.7 eV; above the threshold, a broad feature is centered above 176 eV. The first feature, at 166.5 eV, is fully derived by the L_{3/2} level with an out of the molecular plane (a'') symmetry, while the second one at 167.7 eV is almost completely due to the L_{3/2} level with a symmetry in the molecular plane (a') with a very small contribution from the replica of the 166.5 eV transition due to the L_{1/2} level. Higher-energy features make contributions to both L_{3/2} and L_{1/2} levels with a predominant symmetry in the molecular plane (a').

The S L-edge theoretical spectrum is in good agreement with the experimental one relative to the first two resonances, allowing a clear assignment for these two transitions. However,

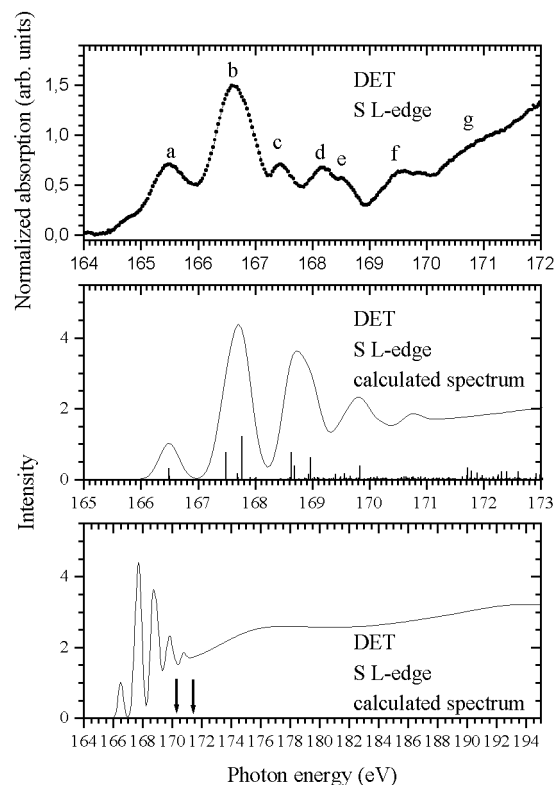


Figure 8. S L-edge spectrum calculated by the STEX method for DET convoluted in the low-energy region with 0.40 eV fwhm Gaussian functions. In the middle panel, the low-energy region is highlighted together with the bar diagram, showing the energy position and intensity of the main STEX transitions. The absolute values of the oscillator strengths (bars) are reported in Table 2. For an easier comparison, in the top panel, the S L-edge experimental spectrum for the low-energy region is also reported.

some differences are observed mainly in the higher-energy region, close to 168 eV.

Hitchcock *et al.* have extensively investigated thiophene,¹² in the gas phase, as a condensed solid, and as a monolayer adsorbed on Pt(111). The S L-edge spectrum for gaseous and solid thiophene closely resembles, in general, the spectrum obtained in this case for DET. These authors detected three main features at 165.6, 166.9, and 168.4 eV assigned to σ^* ($C-S_{3/2}$), overlapping between $\pi_{3/2}^*$ and σ^* ($C-S_{1/2}$), and $\sigma_{3/2}^*$ and $\pi_{3/2}^*$, respectively; the feature at 168.9 eV was assigned to $\sigma_{1/2}^*$. The two resonances detected for DET and labeled “d” and “e” should correspond to these two discussed for thiophene; in this case, the third experimental feature “c” is derived from a new level transition due to the perturbation introduced by the two ethyne groups.

For a thiophene multilayer condensed on an Ag(111) surface,¹³ Vaterlain *et al.* have found three main features in the bound state region at 165.9, 167.2, and 168.5 eV with a general spectral aspect very similar to that reported for thiophene gas;¹² their assignments were in substantial agreement with the previous ones. Vaterlain *et al.*¹³ actually make comments about the relative intensity of the resonance at 167.2 eV, showing the calculation results indicating the overlapping feature derived from the 3/2 and 1/2 components. Depending on the extent of this effect and, therefore, on the energy separation between spin-orbit components, the spectrum can assume a different shape.

The origin of the shoulder that can be detected at 164.8 eV on the low-energy side of the first feature of the experimental S L-edge spectrum is not clear. Vaterlain *et al.*¹³ have detected

a similar feature for the thiophene and 2,2'-bithiophene solid multilayer which was assigned to a transition into the 3b1 (LUMO) orbital. These authors made also some consideration regarding the intensity of this excitation that is dominant in the C K-edge spectrum, and very weak in the sulfur spectrum, concluding that the LUMO possesses predominant 3p character at the sulfur atom.

Conclusions

A photoemission and total-ion-yield NEXAFS investigation of gas-phase diethynylthiophene has been reported as determined experimentally by synchrotron radiation excitation and by calculation.

The photoelectron spectra at the C 1s and S 2p core levels and the total-ion-yield (NEXAFS) spectra at the C K-edge and S L-edge have been experimentally determined. Calculations have been carried out in an effort to obtain the ionization potentials for the C 1s and S 2p core levels by the Δ SCF method and the X-ray absorption cross sections at the C K-edge and S L-edge by the STEX method.

The assignment of the peaks requires the explicit consideration of the interaction of the two different subunits, thiophene and acetylene. The results give a complete picture of the electronic charge perturbation at the α - and β -carbon atoms caused by linking two acetylenes to the thiophene ring.

A general good agreement is observed by comparing experimental and theoretical results, allowing the correct assignment of the experimental features for the C 1s core levels and the C K-edge and S $L_{2,3}$ -edge NEXAFS spectra.

Acknowledgment. G.P. and V.C. thank Italian MIUR and CNR PF-MSTA II for financial support.

References and Notes

- (1) Stokheim, T.; Dekker, M., Eds. *Handbook of Conducting Polymers*; Academic: New York, 1986; Vol. 1 and 2.
- (2) (a) Bredas, J.-L.; Thémans, B.; Fripiat, J. G.; André, J. M.; Chance, R. R. *Phys. Rev. B* **1984**, *29*, 6761. (b) Salaneck, W. R.; Inganäs, O.; Thémans, B.; Nilsson, J. O.; Sjöaren, B.; Osterholm, J. E.; Bredas, J. L.; Svensson, J. J. *Chem. Phys.* **1988**, *89*, 4613.
- (3) Devreux, F.; *et al.* In *Electronic Properties of Conjugated Polymers*; Kuzmany, H., Mehring, M., Roth, S., Eds.; Springer Series in Solid State Sciences, Springer-Verlag: Heidelberg, Germany, 1987; Vol. 76, pp 270.
- (4) Stafström, S. In *Electronic Properties of Conjugated Polymers*; Kuzmany, H., Mehring, M., Roth, S., Eds.; Springer Series in Solid State Sciences, Springer-Verlag: Heidelberg, Germany, 1987; Vol. 76, pp 238.
- (5) (a) Elsembaumer, R. L.; Ken, K. Y.; Miller, G. G.; Shacklette, L. W. *Synth. Met.* **1987**, *18*, 277. (b) Sato, M.; Tanaka, S.; Kaeriyana, K. *Synth. Met.* **1987**, *18*, 229–233.
- (6) Garnier, F.; Hjlouai, R.; Yassar, A.; Srivastava, P. *Science* **1994**, *265*, 1684.
- (7) Garnier, F.; Horowitz, G.; Peng, X.; Fichou, D. *Adv. Mater.* **1990**, *2*, 592.
- (8) Geiger, F.; Stoldt, M.; Bäuerle, P.; Schweizer, H.; Umbach, E. *Adv. Mater.* **1993**, *5*, 922.
- (9) Stoldt, M.; Bäuerle, P.; Schweizer, H.; Umbach, E. *Cryst. Liq. Cryst.* **1994**, *240*, 127.
- (10) Neureiter, H.; Gebauer, W.; Vaterlein, C.; Sokolowski, M.; Bäuerle, P.; Umbach, E. *Synth. Met.* **1994**, *67*, 173.
- (11) (a) Altamura, P.; Giardina, G.; Lo Sterzo, C.; Russo, M. V. *Organometallics* **2001**, *20*, 4360. (b) Giardina, G.; Rosi, P.; Ricci, A.; Lo Sterzo, C. *J. Polym. Sci., Part A: Polym. Chem.* **2000**, *38*, 260.
- (12) Hitchcock, A. P.; Horsley, J. A.; Stöhr, J. *J. Chem. Phys.* **1986**, *85*, 4835.
- (13) Vaterlein, P.; Schmelzer, M.; Taborski, J.; Krause, T.; Viczian, F.; Bäessler, M.; Fink, R.; Umbach, E.; Wurth, W. *Surf. Sci.* **2000**, *452*, 20.
- (14) Baumgärtner, K. M.; Volmer-Uebing, M.; Taborski, J.; Bäuerle, P.; Umbach, E. *Ber. Bunsen-Ges.* **1991**, *95*, 1488.
- (15) Hitchcock, A. P.; Tourillon, G.; Garret, R.; Williams, G. P.; Mahatsekake, C.; Andrieu, C. *J. Phys. Chem.* **1990**, *94*, 2327.

- (16) Ramsey, M. G.; Koller, G.; Karsdinal, I.; Netzer, F. P. *Surf. Sci.* **1996**, *352*, 128.
- (17) Stöhr, J.; Gland, J. L.; Kollin, E. B.; Koestner, R. J.; Johnson, A. L.; Muettterties, E.; Sette, F. *Phys. Rev. Lett.* **1984**, *53*, 2161.
- (18) Stöhr, J.; Kollin, E. B.; Fisher, D. A.; Hastings, J. B.; Zaera, F.; Sette, F. *Phys. Rev. Lett.* **1985**, *55*, 1468.
- (19) Iucci, G.; Polzonetti, G.; Altamura, P.; Paolucci, G.; Goldoni, A.; Russo, M. V. *J. Vac. Sci. Technol., A* **2000**, *18*, 248.
- (20) Ågren, H.; Carravetta, V.; Vahtras, O.; Pettersson, L. G. M. *Chem. Phys. Lett.* **1994**, *222*, 75.
- (21) Domke, M.; Mandel, T.; Puschmann, A.; Xue, C.; Shirley, D. A.; Kaindl, G.; Petersen, H.; Kuske, P. *Rev. Sci. Instrum.* **1992**, *63*, 80.
- (22) Hudson, E.; Shirley, D. A.; Domke, M.; Remmers, G.; Puschmann, A.; Mandel, T.; Xue, C. *Phys. Rev. A* **1993**, *47*, 361.
- (23) Viola, E.; Lo Sterzo, C.; Crescenzi, R.; Frachey, G. *J. Organomet. Chem.* **1995**, *493*, C9–C13.
- (24) Elgaker, T.; Jensen, H. J. A.; Joergensen, P.; Olsen, J.; Ruud, K.; Ågren, H.; Andersen, T.; Bak, K. L.; Bakken, V.; Christiansen, O.; Dahle, P.; Dalskov, E. K.; Enevoldsen, T.; Heiberg, H.; Hettrema, H.; Jonsson, D.; Kirpekar, S.; Kobayashi, R.; Kpoh, H.; Mikkelsen, K. V.; Norman, P.; Packer, M. J.; Saue, T.; Taylor, P. R.; Vahtras, O. *DALTON, an ab initio electronic structure program*, release 1.0, 1997.
- (25) Langhoff, P. W. In *Electron Molecule and Photon Molecule Collisions*; Rescigno, T. N., McKoy, B. V., Schneider, B., Eds.; Plenum: New York, 1979; p 183.
- (26) Gelius, U.; Allan, C. J.; Johansson, G.; Siegbahn, H.; Allison, D. A.; Siegbahn, K. *Phys. Scr.* **1971**, *3*, 237.
- (27) Gelius, U.; Roos, B.; Siegbahn, P. *Chem. Phys. Lett.* **1970**, *4*, 471.
- (28) Clark, D. T.; Lilley, D. M. *Chem. Phys. Lett.* **1971**, *9*, 234.
- (29) Carravetta, V.; Iucci, G.; Ferri, A.; Russo, M. V.; Stranges, S.; De Simone, M.; Polzonetti, G. *Chem. Phys.* **2001**, *264*, 175.
- (30) Polzonetti, G.; Carravetta, V.; Ferri, A.; Altamura, P.; Alagia, M.; Richter, R.; Russo, M. V. *Chem. Phys. Lett.* **2001**, *340*, 449. (30a) *Errata corrigé*: in this paper, the experimental IP values for the C 1s PE spectrum as reported in the table are correct, but unfortunately differ apparently from the figure because of an erroneous energy scale.
- (31) Clark, D. T. *Chem. Commun.* **1971**, 230.
- (32) Tourillon, G.; Jugnet, Y. *J. Chem. Phys.* **1988**, *89*, 1905.
- (33) Plashkevych, O.; Ågren, H.; Carravetta, V.; Contini, G.; Polzonetti, G. *Chem. Phys. Lett.* **2000**, *327*, 7.
- (34) Carravetta, V.; Polzonetti, G.; Iucci, G.; Russo, M. V.; Paolucci, G.; Barnaba, M. *Chem. Phys. Lett.* **1998**, *288*, 37.
- (35) Polzonetti, G.; Carravetta, V.; Russo, M. V.; Contini, G.; Parent, P.; Laffon, C. *J. Electron Spectrosc. Relat. Phenom.* **1999**, *98–99*, 175.